ACS APPLIED MATERIALS & INTERFACES

Research Article

www.acsami.org

Novel Hybrid Structure Silica/CdTe/Molecularly Imprinted Polymer: Synthesis, Specific Recognition, and Quantitative Fluorescence Detection of Bovine Hemoglobin

Dong-Yan Li,[†,‡] Xi-Wen He,[†,‡] Yang Chen,[†,‡] Wen-You Li,[*,†,‡] and Yu-Kui Zhang[†,‡,§]

[†]State Key Laboratory of Medicinal Chemical Biology, and Department of Chemistry, Nankai University, Tianjin 300071, People's Republic of China

[‡]Synergetic Innovation Center of Chemical Science and Engineering (Tianjin), Tianjin 300071, People's Republic of China

[§]National Chromatographic Research and Analysis Center, Dalian Institute of Chemical Physics, Chinese Academy of Sciences, Dalian 116011, People's Republic of China

Supporting Information

ABSTRACT: This work presented a novel strategy for the synthesis of the hybrid structure silica/CdTe/molecularly imprinted polymer (Si-NP/CdTe/MIP) to recognize and detect the template bovine hemoglobin (BHb). First, amino-functionalized silica nanoparticles (Si-NP) and carboxyl-terminated CdTe quantum dots (QDs) were assembled into composite nanoparticles (Si-NP/CdTe) using the EDC (1-(3-dimethylaminopropyl)-3-ethylcarbodiimide hydrochloride) chemistry. Next, Si-NP/CdTe/MIP was synthesized by anchoring molecularly imprinted polymer (MIP) layer on the surface of Si-NP/CdTe through the sol−gel technique and surface imprinting technique. The hybrid structure possessed the selectivity of molecular imprinting technique and the sensitivity of CdTe QDs as well as well-defined morphology. The binding experiment and fluorescence method demonstrated its special recognition performance toward the template BHb. Under the optimized conditions, the fluorescence intensity of the Si-NP/CdTe/MIP decreased linearly with the increase of BHb in the concentration range 0.02−2.1 μM, and the detection limit was 9.4 nM. Moreover, the reusability and reproducibility and the successful applications in practical samples indicated the synthesis of Si-NP/CdTe/MIP provided an alternative solution for special recognition and determination of protein from real samples.

KEYWORDS: *molecularly imprinted polymer, quantum dots, fluorescent detection, protein recognition*

1. INTRODUCTION

Molecular imprinting is a well-known technique for the creation of tailor-made binding sites with memory of the shape, size, and functional groups of the template.[1] Synthesizing molecularly imprinted polymer (MIP) involves the copolymerization of functional monomers and cross-linkers in the presence of the template, and the special tailor-made binding sites are exposed after the removal of the template. Thus, MIP has two characteristics of the most important features: the ability of recognition and binding special target molecules.[2] Recently, MIP has become very attractive and been applied in the fields of chem/biosensor,[3,4] extraction/separation,[5] catalysis,[6] antibody mimetics,[7] and drug delivery[8] owing to its desired selectivity, physical robustness, good stability, and low cost and reusability.[1]

Although the synthesis of MIP toward small molecules is straightforward now, the imprinting of biomacromolecules like proteins continues to be a significant challenge.[9,10] The difficulties faced by proteins for imprinting applications lie in their large molecular size, diffusion limitation, complexity, flexible conformation, and solubility.[11] To overcome these problems, a surface imprinting technique has been adopted to various support materials (e.g., silica nanoparticles,[12] silica nanotubes,[13] alumina membrane,[14] and magnetic nanoparticles[15]). Particularly, silica nanoparticles are popular substrates for imprinted MIP for many reasons including: (a) the synthesis of silica nanoparticles themselves is a well-established process; (b) silica possesses numerous hydroxyl groups on its surface and was employed as grafting sites for the surface polymer; (c) the chemical/mechanical stability, nontoxicity, and biocompatibility of silica make it an attractive substrate in many fields.[16] The introduction of the thin imprinted layer coating on the surface of silica nanoparticles via surface imprinting enables the elution and rebinding of the target template easily. Meanwhile, the selective recognition and determination of proteins in biological samples

Received: September 11, 2013
Accepted: November 20, 2013
Published: November 20, 2013

   dx.doi.org/10.1021/am403942y | ACS Appl. Mater. Interfaces 2013, 5, 12609−12616

are of great significance in life science. Hence, photoluminescence materials (e.g., QDs) have been proposed as feasible strategies for synthesizing MIP.

QDs are often described as "artificial atoms", exhibiting unique luminescence characteristics and electronic properties such as wide and continuous absorption spectra, narrow emission spectra, and high light stability.[17,18] Therefore, some MIPs have been synthesized by encapsulating QDs in cross-linked polymers combining the selectivity of molecular imprinting technology and the sensitivity of QDs.[19,20] For example, Yan's group has developed a type of MIP-based room-temperature phosphorescence by anchoring a MIP layer on the surface of Mn-doped ZnS QDs for detecting pentachlorophenol.[20] Wang's group has introduced a fluorescence nanosensing material by anchoring the MIP layer on 1-vinyl-3-octylimidazolium ionic liquid-modified CdSe/ZnS QDs for optosensing of tocopherol.[21] Our group has developed a series of protein-imprinted polymers by encapsulating CdTe QDs into silicon material, in which the synthesis of MIPs was under the condition of water phase and the morphology of MIPs still left much to be desired.[22−24] The reasons could be explained that because the size of QD is small, some of the imprinted outer layers would actually be coated on QD aggregates comprised of several QDs and the shape of MIP was aggregated.[25−27] To improve the morphology of MIP and possess a favorable fluorescence spectrum simultaneously, Chen's group proposed a novel approach for creating MIP-capped QDs sensing for imprinting 2,4,6-trinitrotoluene by a seed-growth method via a sol−gel process.[4] On the basis of these studies, a novel strategy for synthesizing a unique hybrid structure for imprinting target protein was proposed. The Si-NP/CdTe/MIP was constructed by the sol−gel technique and surface molecular imprinting technique, combining the merits of MIP and QDs as well as well-defined morphology. The hybrid structure possessed multifunctional properties for selective recognition, separation, and detection of protein from complex samples.

In this work, carboxyl-terminated CdTe QDs and amino-functionalized silica nanoparticles were first assembled into Si-NP/CdTe by covalently linking the highly fluorescent CdTe QDs on the surface of the Si-NP. Numerous "satellites" of QDs were linked on the surface of the Si-NP by the way of amide bonding that owned photoluminescence properties and played the role of well-defined support substrates for nanostructured imprinted materials by the surface imprinting technique. And then, the MIP layer was anchored on the surface of Si-NP/CdTe to form the unique Si-NP/CdTe/MIP, which possessed the high selectivity of molecular imprinting technology (MIT) and the high sensitivity of CdTe QDs. Besides, the Si-NP/CdTe/MIP provided better site accessibility, lower mass transfer resistance for special recognition, and detection performance toward the corresponding template protein. Moreover, the reusability and reproducibility as well as the successful applications in practical samples indicated the approach for synthesizing Si-NP/CdTe/MIP provided an alternative solution for special recognition and detection of protein.

2. EXPERIMENTAL SECTION

2.1. Materials. All reagents used were of at least analytical grade. Tellurium powder, $CdCl_2·2.5H_2O$, $NaBH_4$, ammonium hydroxide ($NH_3·H_2O$), (2-*N*-morpholino)ethanesulfonic acid (MES), 3-aminopropyltriethoxysilane (APTES), and tetraethoxysilicane (TEOS) were obtained from J & K Chemical Co. 3-Mercaptopropionic acid (MPA) was purchased from Alfa Aesar. Triton X-100 was purchased from Solarbio Co. Bovine hemoglobin (BHb, p*I* (isoelectric point) = 6.9, MW (molecular weight) = 64.5 kDa), bovine serum albumin (BSA, p*I* = 4.9, MW = 66.0 kDa), lysozyme (Lyz, p*I* = 11.0, MW = 14.4 kDa), ovalbumin (OB, p*I* = 4.7, MW = 45.0 kDa), and 1-(3-dimethylaminopropyl)-3-ethylcarbodiimide hydrochloride (EDC) were purchased from Sigma. Bovine blood was kindly gifted by Xiaochuan Biotech. Co. Ltd. (Tianjin, China). The urine was collected from a healthy volunteer.

2.2. Characterization. Fluorescence (FL) measurements were performed on an F-4500 fluorospectrophotometer (Hitachi). UV−vis spectra (200−800 nm) were recorded on a UV-2450 spectrophotometer (Shimadzu). Fourier-transform infrared (FT-IR) spectra (4000−400 cm^{-1}) in KBr were recorded by using a Vector 22 FT-IR spectrophotometer (Bruker). The morphologies and sizes of samples were obtained by field-emission scanning electron microscope (FESEM, JSM-7500F, JEOL) and high-resolution transmission electron microscope (HRTEM, Tecnai G^2 F20, Philips). Energy dispersive X-ray (EDS, Oxford, Britain) was used to analyze the chemical elements on the surface of samples. X-ray photoelectron spectroscopy (XPS) measurements were performed with an ESCALAB 250 spectrometer (Thermo-VG Scientific) with ultrahigh vacuum generators. Gel electrophoresis was carried out by sodium dodecyl sulfate polyacrylamide gel electrophoresis (SDS-PAGE) with 18% running gel and 6% stacking gel (Bio-Rad).

2.3. Synthesis of Carboxyl-Terminated CdTe QDs. The carboxyl-terminated CdTe QDs were synthesized according to previous reports with some modifications.[28] Briefly, after tellurium powder was reduced completely by excessive $NaBH_4$, 1.5 mL of a freshly prepared NaHTe(aq) solution was injected into a $CdCl_2$−MPA solution, which was deaerated by N_2 for 30 min. The molar ratio of Cd^{2+}/HTe^{-}/MPA was set as 1:0.5:2.4. Then the solution was heated up until boiling. After the solution was refluxed for 2 h, the MPA stabilized CdTe QDs were obtained.

2.4. Synthesis of Amino-Functionalized Si-NP. Amino-functionalized silica nanoparticles (Si-NP) were synthesized based on a modified Stöber method.[29,30] Fifty milliliters of ethanol and 50 mL of water were added to a 250 mL round-bottomed flask with a mechanical stirring bar. Ten milliliters of $NH_3·H_2O$ was added, and the mixture was stirred at 600 rpm. Five milliliters of TEOS was added drop by drop, and then the resultant mixture was stirred overnight. Five milliliters of APTES was then added, and the mixed solution was stirred for an additional 12 h. The amino-functionalized silica nanoparticles were centrifuged and washed with ethanol at least five times before being dried under vacuum.

2.5. Fabrication of Si-NP/CdTe. Ten milligrams of Si-NP were dispersed in 20 mL of MES buffer (0.1 mmol); meanwhile, EDC (20 mg/mL) was dispersed in CdTe(aq) solution. After the carboxyl groups were activated, CdTe QDs were added drop by drop into the solution of Si-NP.[31,32] The final mixture was stirred for 12 h at room temperature in the dark. Finally, the Si-NP/CdTe composite nanoparticles were centrifuged at 13 000 rpm for 5 min for three times (unbound QDs were removed) and then washed with phosphate buffer saline (PBS) (0.01 mol/L, pH 7.0).

2.6. Preparation of Si-NP/CdTe/MIP. The Si-NP/CdTe nanoparticles were dispersed in 20 mL of PBS buffer solution (0.01 mol/L, pH 7.0), in which 80 μL of APTES and 10 mg of BHb were added and stirred for 30 min. And then, 100 μL of TEOS and 100 μL of $NH_3·H_2O$ were added and stirred for 2h. Finally, the Si-NP/CdTe/MIP nanoparticles that owned specific imprinted cavities were obtained after the removal of embedded template protein BHb. Briefly, 20 mL of 0.5% Triton X-100 solution was added to the resultant polymers and the mixture was stirred about 1 h at room temperature, and then the polymers were centrifuged at 13 000 rpm for 5 min and washed with 0.5% Triton X-100 until no template protein was detected by the UV−vis spectrophotometer at 406 nm. The nonimprinted polymer (Si-NP/CdTe/NIP) was prepared under the same conditions in the absence of the template.

2.7. Binding Experiment. The adsorption experiment was performed to evaluate the binding capacity of the Si-NP/CdTe/MIP. Thirty milligrams of Si-NP/CdTe/MIP and Si-NP/CdTe/NIP were added to 3 mL of 0.2 mg/mL BHb solution (0.01 mol/L PBS, pH 7.0)

Scheme 1. Illustration for the Preparation of the Si-NP/CdTe/MIP and the Fluorescence Quenching Detection of BHb upon Specific Recognition

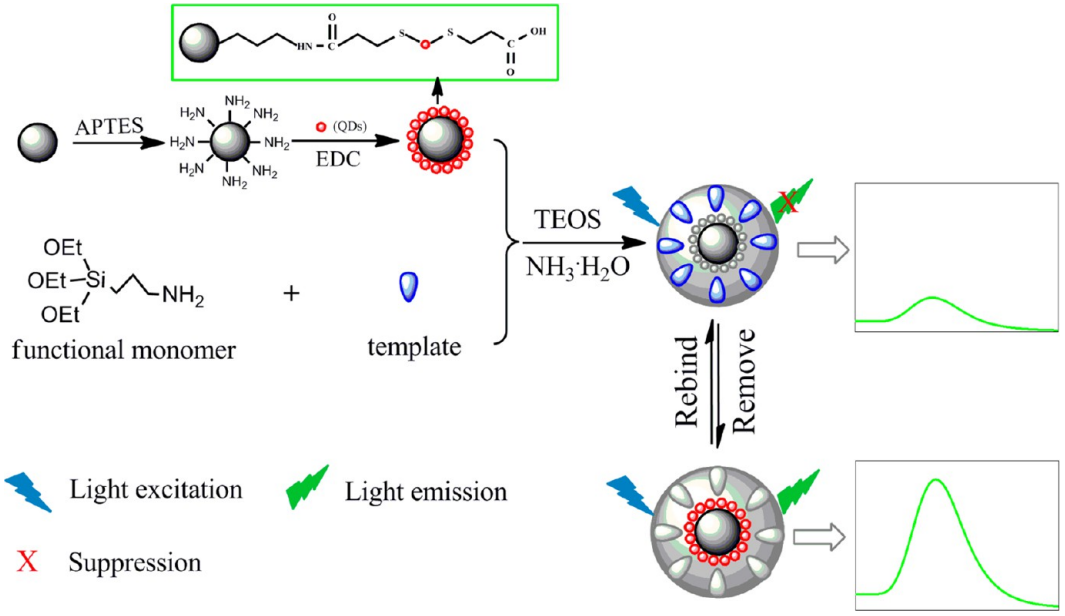

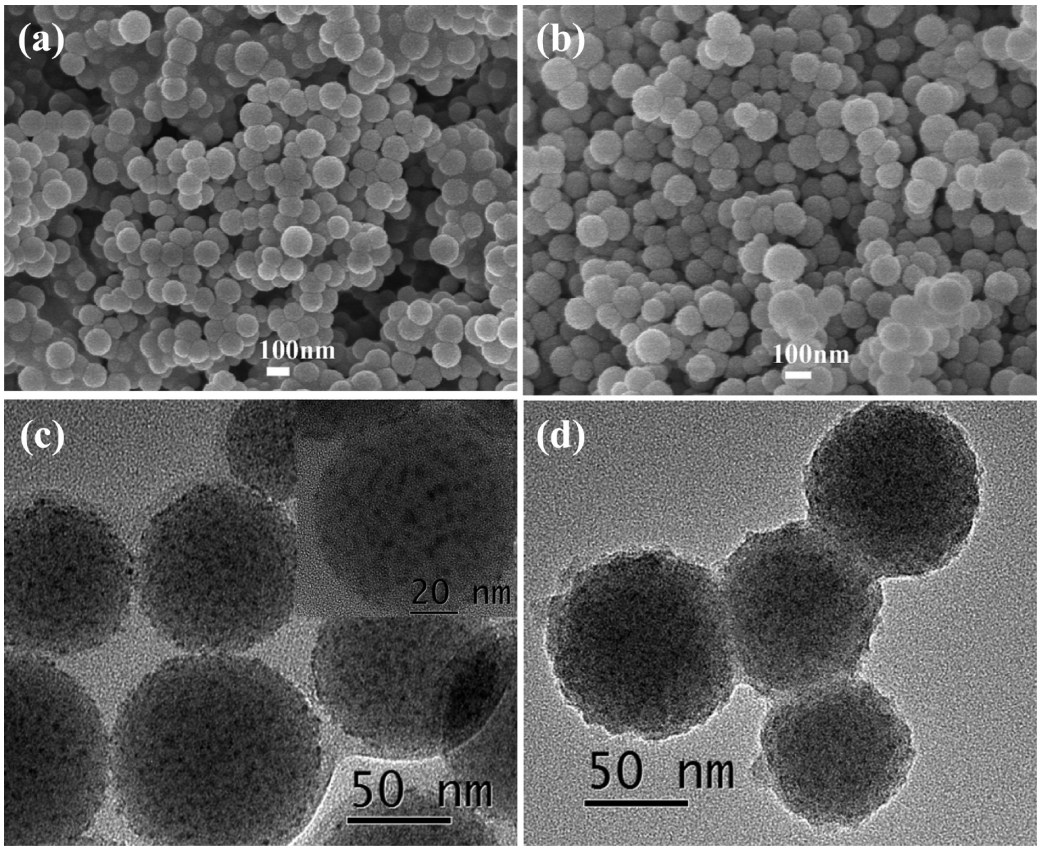

Figure 1. (a) FESEM image of Si-NP, (b) FESEM and (c) HRTEM images of Si-NP/CdTe (inset: high magnification HRTEM image of Si-NP/CdTe), and (d) HRTEM image of Si-NP/CdTe/MIP.

respectively, and placed on the table concentrator. The supernatant and polymers were separated by centrifugation and detected by the UV−vis spectrophotometer. The adsorption capacity (Q) is calculated using the equation below:

$$Q = (C_0 - C_t)V/W(\mathrm{mg\,g^{-1}}) \quad (1)$$

where C_0 and C_t are the initial and equilibrium concentrations of the template protein BHb, respectively, V (mL) is the volume of the initial solution, and W (g) is the weight of the Si-NP/CdTe/MIP.

2.8. Fluorescence Measurement. In the experiment, all the fluorescence (FL) intensity detections were under the same conditions: the slit widths of the excitation and emission were both 10 nm, and the excitation wavelength was set at 450 nm with a recording emission range

of 490−700 nm. The photomultiplier tube voltage was set at 700 V. The appropriate Si-NP/CdTe/MIP or Si-NP/CdTe/NIP solution was added to a 5 mL standard colorimetric tube, and the given concentration of protein was added successively. The mixture was mixed thoroughly and scanned by the F-4500 fluorospectrophotometer.

2.9. Bovine Blood and Urine Samples. Bovine blood and urine samples were used to demonstrate the applicability of the Si-NP/CdTe/MIP nanomaterial for specific recognition and quantitative fluorescence detection of BHb. Briefly, the bovine blood sample was diluted 300-fold with PBS buffer (0.01 mol/L, pH 7.0), and then 6 mg of Si-NP/CdTe/MIP and Si-NP/CdTe/NIP were immerged with 400 μL of 300-fold dilution of bovine blood, respectively. And then, the Si-NP/CdTe/MIP and Si-NP/CdTe/NIP were washed with PBS buffer (0.01 mol/L, pH 7.0) to remove nonspecific binding proteins. Next, 0.5% Triton X-100 was employed to elute the specifically adsorbed BHb. Finally, 20 μL of each sample was used for SDS-PAGE analysis.

Both a 100-fold dilution of urine and a 6000-fold dilution of bovine blood were used to detect and assess the analysis method and the accuracy of the measurement system. As no BHb in the collected urine was detectable by the method, the recovery was carried out by the standard addition method with 5.0×10^{-7} to 15.0×10^{-7} mol/L BHb. Also, the detection of BHb in the bovine blood sample was performed based on the premise that the concentration of BHb in 6000-fold dilution of bovine blood was in the linear range, and then the recovery was performed by the spiked BHb.

3. RESULTS AND DISCUSSIONS

3.1. Preparation and Characterization of the Hybrid Structure. The Si-NP/CdTe/MIP was prepared via a multistep procedure (Scheme 1). In this protocol, the monodispersed silica nanoparticles were prepared by the Stöber method and subsequently modified with APTES to form the amino-functioned Si-NP.[33] MPA on the surface of CdTe QDs acted as a stabilizer and provided carboxyl groups for conjugating with amino-functionalized. Next, the copolymerization of the composited Si-NP/CdTe, APTES (functional monomer), template (BHb), and TEOS (cross-linking agent) formed polymeric network around the template. Finally, the Si-NP/CdTe/MIP that owned specific imprinted cavities were obtained after the removal of embedded template protein BHb.

As shown in Figure S1 (Supporting Information), the size of the CdTe QDs was about 3 nm. The particle size of uniform Si-NP was about 90 nm (Figure 1a). After CdTe QDs were linked around the Si-NP surfaces, FESEM analysis showed that the resultant Si-NP/CdTe nanoparticles were highly spherical in shape and uniform in size (Figure 1b), which played the role of well-defined support substrates for nanostructured imprinted materials. Because the particle size of the CdTe QDs was only about 3 nm (as shown in Figure S1, Supporting Information), no obvious change can be observed from the FESEM image of the Si-NP/CdTe. However, CdTe QDs being linked outside the Si-NP surface can be seen from the HRTEM image of Si-NP/CdTe (Figure 1c). After the MIP layer was anchored on the Si-NP/CdTe, it was observed from Figure 1d that the thin molecularly imprinted layer was about 10 nm in the outmost layer, which provided better site accessibility, lower mass transfer resistance, and well-defined material shape for special recognition toward the corresponding template protein.[34] The result indicated that the hybrid structure was successfully synthesized, and it owned Si-NP as the support substrates, the CdTe QDs with the fluorescence properties and the thin molecularly imprinted layer for specific recognition of protein.

To further confirm the successful synthesis of the hybrid structure, EDS and XPS spectroscopy analysis were employed. As shown in Figure S2A (Supporting Information), the signal of N (Kα) at 0.392 keV appeared, indicating the amino group was successfully modified onto the surface of the Si-NP. And then, it can be seen from Figure S2B (Supporting Information) that the hybrid structure owned the elements of Cd (Lα) at 3.124 keV and Te (Lα) at 3.769 keV, which confirmed that CdTe QDs were successfully modified on the surface of the Si-NP. The XPS spectrum of the as-prepared hybrid structure was also recorded to analyze the surface chemical compositions and gain more structure information (Figure S3, Supporting Information). In the spectrum, the elements of Si, N, C, and O could be clearly seen. The signals of Cd and Te are very weak, which indicated CdTe QDs were embedded in the inside of MIP layer and only a trace amount of them was detected.

FT-IR spectra were further investigated and are shown in Figure S4 (Supporting Information). The characteristic signals of the stretching vibration of Si−O−Si at 1087 cm^{-1} and Si−O vibration at 794 cm^{-1} and amino group of APTES at 3414, 1641, and 1618 cm^{-1} were observed in the spectrum of Si-NP (Figure S4b, Supporting Information), which proved the amino groups were successfully modified onto the surface of silica nanoparticles. The successful synthesis of Si-NP/CdTe composite nanoparticles was further studied as shown in Figure S4c (Supporting Information), which had a peak at 1400 cm^{-1} due to the vibration of CO-NH, and the peak at 1560 cm^{-1} of Figure S4a (Supporting Information) reappeared. Because there is no introduction of new functional groups, compared with Figure S4c (Supporting Information), the spectrum of Si-NP/CdTe/MIP had no obvious change and was shown in Figure S4d (Supporting Information).

3.2. Adsorption Properties of Si-NP/CdTe/MIP. *3.2.1. Adsorption Capacity.* To investigate the binding affinity of Si-NP/CdTe/MIP and Si-NP/CdTe/NIP, the adsorption test was performed by adsorbing the template BHb. The adsorption capacity of Si-NP/CdTe/MIP and Si-NP/CdTe/NIP are shown in Figure 2. In this case, the experimental adsorption capacity of

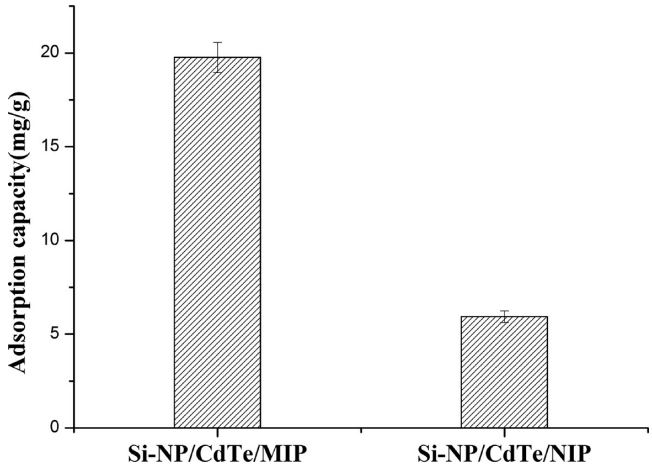

Figure 2. The adsorption capacity of Si-NP/CdTe/MIP and Si-NP/CdTe/NIP.

the Si-NP/CdTe/MIP was 19.7 mg/g. Different from Si-NP/CdTe/MIP, the Si-NP/CdTe/NIP showed a low binding affinity toward the protein BHb and the adsorption capacity was 5.9 mg/g. The result could be explained that special cavities of BHb were formed during the imprinting process and the Si-NP/CdTe/MIP showed higher binding affinity for BHb. On the contrary, as for Si-NP/CdTe/NIP, there was lack of recognition sites and the

nonspecific adsorption had a dominant effect. Therefore, its adsorption capacity was low.

3.2.2. Adsorption–Desorption and Reproducibility. Desorption and regeneration are important indicators for the application of the Si-NP/CdTe/MIP nanomaterial. The adsorption–desorption cycles were repeated six times using the same batch of Si-NP/CdTe/MIP and Si-NP/CdTe/NIP to study their reversible binding and release behavior. As shown in Figure 3, it could be seen that the adsorption capacity of the Si-NP/CdTe/MIP lost about 8.5% of its affinity on average over six cycles and the Si-NP/CdTe/NIP had no obvious change. It is possible that some specific cavities were blocked during the process of adsorption or destroyed after rewashing. On the contrary, the Si-NP/CdTe/NIP had no imprinted recognition site, and the washing was insignificant. The results indicated that Si-NP/CdTe/MIP and Si-NP/CdTe/NIP retained their recovery efficiency, which was a clear superiority over disposable materials and could be used repeatedly at least within six cycles.

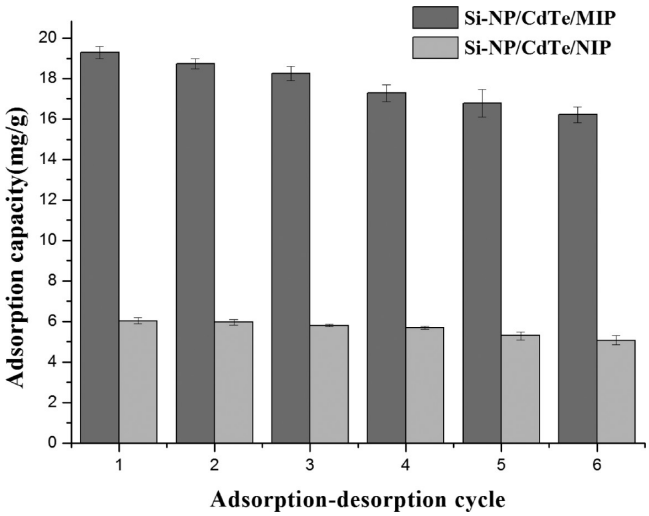

Figure 3. Adsorption–desorption ability of Si-NP/CdTe/MIP and Si-NP/CdTe/NIP.

Reproducibility is also important for the Si-NP/CdTe/MIP as a performing material. The reproducibility experiment was studied by using six different batches of Si-NP/CdTe/MIP and Si-NP/CdTe/NIP prepared at different times. Through three parallel determinations to every batch, the result showed that the reproducibilities of Si-NP/CdTe/MIP and Si-NP/CdTe/NIP were all satisfactory with a RSD less than 5%.

3.3. Optosensing of BHb by the Si-NP/CdTe/MIP. *3.3.1. Influence of Monomer and Cross-linking Agent.* To synthesize the effective and favorable molecularly imprinted polymer, the amount of functional monomer APTES and cross-linking agent TEOS were investigated (Figure S5, Supporting Information). The quenching amount, defined as $(F_0/F)-1$, was used as the index of the quenching capacity. As shown in Figure S5a (Supporting Information), the FL intensity of Si-NP/CdTe/MIP gradually decreased with increasing the amount of APTES, which it is possible that the native structure of CdTe QDs was destroyed by APTES during the process of fabricating the silica shell onto the Si-NP/CdTe composite nanoparticles. According to the quenching amount and the FL intensity of Si-NP/CdTe/MIP, 80 μL of APTES was chosen as the appropriate amount for the further experiments. On the basis of the same principle, 100 μL of TEOS was selected as the cross-linking agent for performing the fluorescent sensor (Figure S5b, Supporting Information).

3.3.2. Effect of pH and the Stability. The pH plays an important role in determining the structure of the sol–gel-derived polymer and has obvious effects on the activity and the charge of BHb as well as the FL intensity of Si-NP/CdTe/MIP.[35] As shown in Figure 4, the effects of pH on the quenching amount of the Si-NP/CdTe/MIP are more obvious than that of the Si-NP/CdTe/NIP. That was because the tailor-made binding sites were formed in Si-NP/CdTe/MIP, and pH affected three-dimensional structure proteins and hence affected BHb rebinding at different pH. Besides, the synthesis of CdTe QDs was under the alkaline, and the FL intensity was low under the condition of the pH less than 7. However, with the increase of pH, the quenching amount of Si-NP/CdTe/MIP decreases quickly because the molecular imprinting silica layer can be ionized at high pH, which would affect the interaction between the template protein and the fluorescent sensor. Above all, BHb may be denatured under high or low pH. Combining the quenching amount of Si-NP/CdTe/MIP and the physiological condition, 0.01 mol/L PBS buffer (pH 7.0) was selected as the optimized binding media for further experiments.

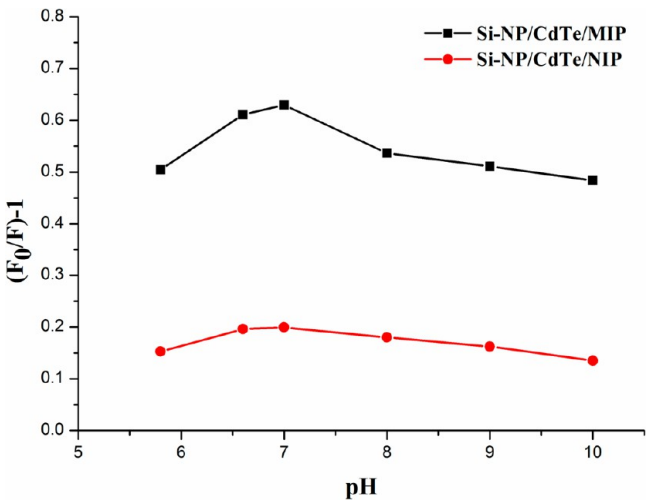

Figure 4. The pH-dependent FL intensity changes of Si-NP/CdTe/MIP and Si-NP/CdTe/NIP by template BHb.

Under the optimized conditions, the fluorescence stability was evaluated by the repeated detections of the fluorescence intensity of Si-NP/CdTe/MIP every 10 min. As shown in Figure 5, the change of the FL intensity of Si-NP/CdTe/MIP was not obvious, which showed a stable emission of Si-NP/CdTe/MIP within 60 min. And then, the change of fluorescence intensity during the storage of Si-NP/CdTe/MIP was also investigated (Figure S6, Supporting Information). When the sensor was stored for 7 days, the fluorescence intensity retained 91% of its original response, which indicated the unique sensor has acceptable storage stability. These results might demonstrate that the molecularly imprinted layer was effectively anchored on the surface of Si-NP/CdTe, and the CdTe QDs were well protected by the molecularly imprinted layer.

3.3.3. Si-NP/CdTe/MIP with BHb of Different Concentrations. To study the binding affinity properties of Si-NP/CdTe/MIP and Si-NP/CdTe/NIP with the template BHb, the fluorescence analysis was carried out. The fluorescence quenching followed the Stern–Volmer equation.

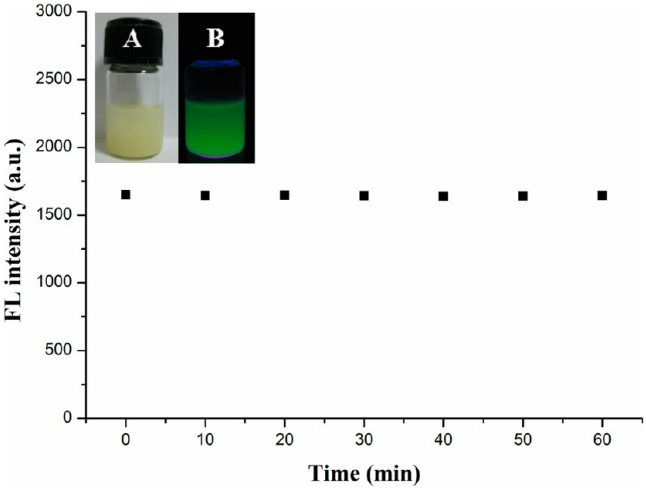

Figure 5. Fluorescence intensity change of Si-NP/CdTe/MIP within 60 min. Inset: fluorescence photographs of Si-NP/CdTe/MIP in PBS buffer solution under visible light (A) and under UV light irradiation (B).

$$F_0/F = 1 + K_{SV}[Q] \quad (2)$$

F_0 and F were the FL intensity of CdTe QDs in the absence and presence of the template, respectively, K_{SV} was the Stern–Volmer constant, and [Q] was the concentration of BHb. The ratio of $K_{SV,MIP}$ to $K_{SV,NIP}$ was defined as the imprinting factor (IF).

As shown in Figure 6, the FL intensity of the Si-NP/CdTe/MIP and Si-NP/CdTe/NIP decreased linearly with the increase of the concentrations of BHb. It was seen that the decrease of FL intensity of the Si-NP/CdTe/MIP was much larger than that of Si-NP/CdTe/NIP at the same concentration of BHb, which was because specific molecular recognition sites of predetermined selectivity were formed in the Si-NP/CdTe/MIP; however, the Si-NP/CdTe/NIP had no imprinting cavity. Under the optimized conditions, the fluorescence intensity of the Si-NP/CdTe/MIP decreased linearly with the increase of the template protein BHb in the concentration range 0.02–2.1 μM, and the detection limit was 9.4 nM. On the basis of the quenching amount of the FL intensity of Si-NP/CdTe/MIP with BHb, the Si-NP/CdTe/MIP as a fluorescent sensor was used to detect template protein. The precision for five replicate detections of BHb at 0.20 μM was 0.98% (relative standard deviation), and the imprinting factor (IF) was 3.79, which indicates that the Si-NP/CdTe/MIP can recognize the template BHb.

3.3.4. Selective and Competitive Binding. The fluorescent response of Si-NP/CdTe/MIP toward various proteins was performed to study its selectivity toward the template. As shown in Figure 7a, Si-NP/CdTe/MIP had a strong response to BHb, which caused a significant change of FL intensity with a high quenching amount, more obvious than other proteins. In the process of synthesis of the Si-NP/CdTe/MIP, many specific imprinted cavities with the memory of the shape, size, and functional groups of BHb were generated. Although Lyz and OB were small to get into the cavities, the specific recognition sites were not complementary to Lyz and OB, thus they are not easy to quench the fluorescence of the Si-NP/CdTe/MIP. As for BSA, although its molecular weight was similar with BHb, it could not be completely matched with the preparative imprinted sites of BHb. Therefore, BSA also could not effectively quench the fluorescence of the Si-NP/CdTe/MIP.

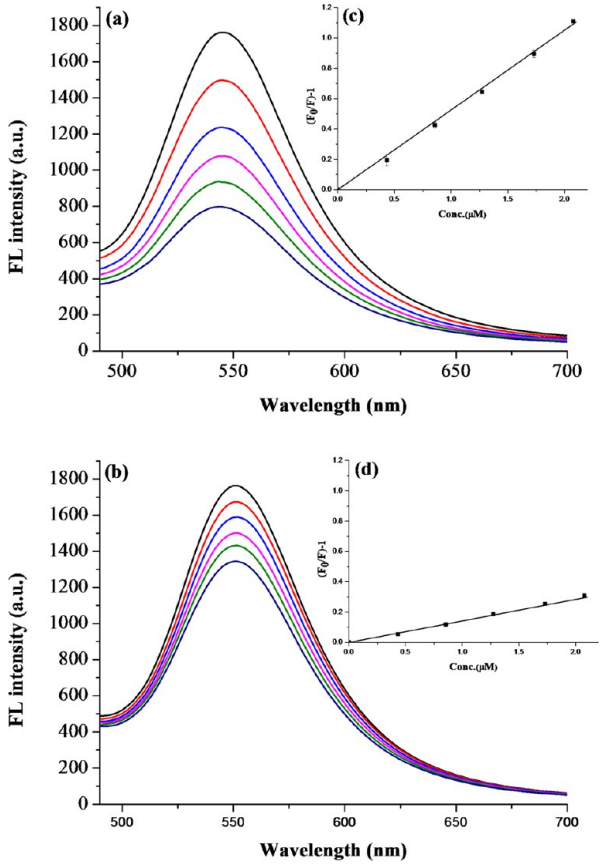

Figure 6. Fluorescence emission spectra of Si-NP/CdTe/MIP (a) and Si-NP/CdTe/NIP (b) with addition of the indicated concentrations of BHb. The Stern–Volmer plots of Si-NP/CdTe/MIP (c) and Si-NP/CdTe/NIP (d) with BHb, respectively.

The competitive binding experiments were performed by changing the ratio of different concentrations of BSA and the fixed concentration of BHb. As shown in Figure 7b, the FL intensity of Si-NP/CdTe/MIP had no significant change with the increase of the C_{BSA}/C_{BHb} ratio. The result can be explained that although BSA has a molecular weight similar to BHb, BHb is a tetrameric protein composed of pairs of two different polypeptides and has a biconcave shape, and the size of hemoglobin is about 65 Å; BSA consists of one polypeptide and has an ellipsoidal shape, and the size of BSA is about 154 Å, larger than BHb.[36] Therefore, BSA did not match with the special recognition sites, and it could not effectively quench the fluorescence intensity of the Si-NP/CdTe/MIP. Through the competitive experiments, it was further confirmed that the Si-NP/CdTe/MIP had the specific recognition toward BHb.

3.4. Analysis and Detection of BHb in Real Samples. The practicability of Si-NP/CdTe/MIP was evaluated by selective separation and enrichment of BHb from bovine blood, and the SDS-PAGE was used to visualize protein samples. As presented in Figure 8, the bands of BHb and BSA appeared in 300-fold dilution of bovine blood without treatment (lane 1). Lane 2 showed the supernatant after treatment with Si-NP/CdTe/MIP, in which hardly any BHb was left. Namely, almost all of the BHb was captured by Si-NP/CdTe/MIP. After elution with Triton X-100, the band of BHb reappeared in lane 4, indicating BHb was enriched. Compared with Si-NP/CdTe/MIP, lanes 3 and 5 showed the supernatant after treatment with Si-NP/CdTe/NIP and the corresponding eluent with Triton X-

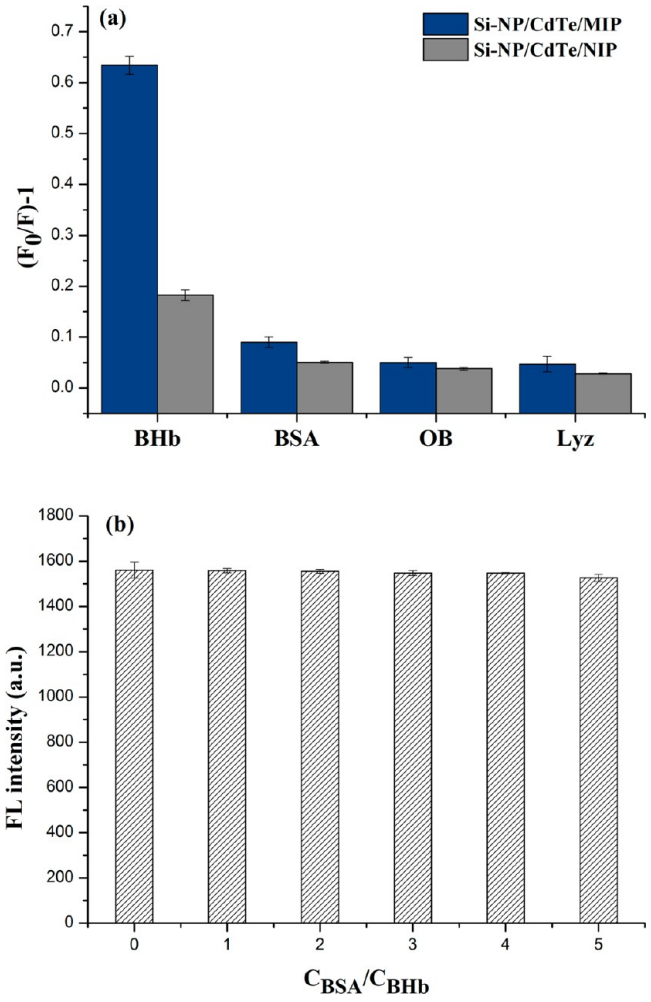

Figure 7. (a) Binding behaviors of different proteins (1.25 μM) on the Si-NP/CdTe/MIP and Si-NP/CdTe/NIP. (b) Effects of the special competitive protein BSA on the binding capacity under the different concentration of BSA and the fixed concentration of BHb (1.25 μM) on the Si-NP/CdTe/MIP.

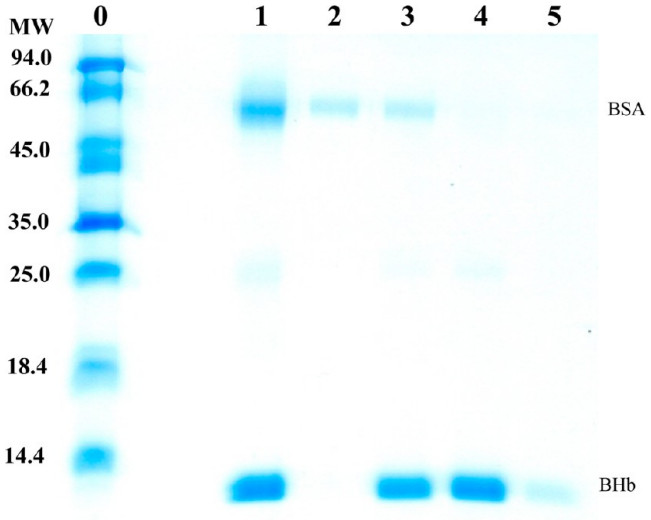

Figure 8. SDS-PAGE analysis of bovine blood samples before and after treatment by Si-NP/CdTe/MIP and Si-NP/CdTe/NIP: lane 0, protein marker; lane 1, 300-fold dilution of bovine blood before treatment; lane 2, the supernatant after treatment with Si-NP/CdTe/MIP; lane 3, the supernatant after treatment with Si-NP/CdTe/NIP; lane 4, the eluent from Si-NP/CdTe/MIP; lane 5, the eluent from Si-NP/CdTe/NIP.

Table 1. Results for the Determination of the BHb in 100-fold Dilution of Urine and 6000-fold Dilution of Bovine Blood

	BHb concentration (10^{-7} M)		
sample	spiked	measured[a]	%[b]
urine	0.0	nd[c]	
	5.0	5.1 ± 0.1	102.0 ± 2.0
	10.0	10.1 ± 0.2	100.5 ± 4.0
	15.0	14.8 ± 0.3	98.7 ± 2.0
bovine blood	0.0	1.9 ± 0.1	
	5.0	7.1 ± 0.3	104.0 ± 2.0
	10.0	11.9 ± 0.6	100.0 ± 6.0
	15.0	16.5 ± 0.5	97.3 ± 3.3

[a]mean ± std, n = 3. [b]mean ± std recovery %, n = 3. [c]Not detected.

100. From lane 3, we can see about 75% BHb (quantification of the protein bands was performed with Quantity One software (Bio-Rad)) still existed in the supernatant after treatment with Si-NP/CdTe/NIP. The results further illustrated that the specific recognition sites were formed in Si-NP/CdTe/MIP and it has potential application for the selective separation and enrichment of BHb in biological samples.

Specific and sensitive detection of proteins in practical and biological samples is also one of the most important goals.[37] To confirm the ability of the strategy to sensitively detect the target protein from real complex biological fluids, urine and bovine blood were chosen and detected by the developed Si-NP/CdTe/MIP method. First, the 100-fold dilution of urine was used to detect and assess the analysis method and the accuracy of the measurement system. As shown in Table 1, the recovery of the 100-fold dilution of urine sample was 98.7%−102.0%. And then, we spiked different concentrations of BHb into the 6000-fold dilution of bovine blood, attaining a recovery of 97.3%−104.0%. Overall, the result showed the fluorescent sensor was successfully applied in the detection of BHb in biological samples.

4. CONCLUSIONS

In this work, a novel strategy was explored for the preparation of the Si-NP/CdTe/MIP that possessed CdTe QDs as the fluorescence species and silica nanoparticles as the support substrate for surface imprinting. The fluorescent Si-NP/CdTe/MIP integrated the high sensitivity of QDs and the high selectivity of MIT as well as the well-defined morphology and was successfully used for the selective recognition and determination of the template BHb in the biological samples. The approach for synthesizing the Si-NP/CdTe/MIP sensor provided an alternative solution for special recognition and determination of protein in biological fluids as well as might applied in more fields involving bio-diagnostics, biomedical and proteomics research.

■ ASSOCIATED CONTENT

Supporting Information

HRTEM images of CdTe QDs with different scales, EDS spectra of Si-NP and Si-NP/CdTe, XPS spectrum of the as-prepared Si-NP/CdTe/MIP, and FT-IR spectra of CdTe QDs, amine-modified Si−NP, Si-NP/CdTe, and Si-NP/CdTe/MIP. Graph plots showing the effects of the amount of functional monomer

APTES and the cross-linking agent TEOS on fluorescence intensity of Si-NP/CdTe/MIP and the quenching amount of Si-NP/CdTe/MIP with the protein BHb, and plots showing fluorescence intensity change of Si-NP/CdTe/MIP within 7 days (storage in a dark environment). This material is available free of charge via the Internet at http://pubs.acs.org.

AUTHOR INFORMATION

Corresponding Author

*W.-Y. Li. E-mail: wyli@nankai.edu.cn.

Notes

The authors declare no competing financial interest.

ACKNOWLEDGMENTS

This work was supported by the National Basic Research Program of China (973 Program) (Nos. 2011CB707703 and 2012CB910601), the National Natural Science Foundation of China (No. 21075069 and 21275078), and the Tianjin Natural Science Foundation (No. 11JCZDJC21700).

REFERENCES

(1) Chen, L.; Xu, S.; Li, J. *Chem. Soc. Rev.* **2011**, *40*, 2922−2942.
(2) Haupt, K. *Nat. Mater.* **2010**, *9*, 612−614.
(3) Lee, M. H.; Thomas, J. L.; Ho, M. H.; Yuan, C.; Lin, H. Y. *ACS Appl. Mater. Interfaces* **2010**, *2*, 1729−1736.
(4) Xu, S.; Lu, H.; Li, J.; Song, X.; Wang, A.; Chen, L.; Han, S. *ACS Appl. Mater. Interfaces* **2013**, *5*, 8146−8154.
(5) Lee, M. H.; Thomas, J. L.; Chen, Y. C.; Wang, H. Y.; Lin, H. Y. *ACS Appl. Mater. Interfaces* **2012**, *4*, 916−921.
(6) Volkmann, A.; Brüggemann, O. *React. Funct. Polym.* **2006**, *66*, 1725−1733.
(7) Hoshino, Y.; Koide, H.; Urakami, T.; Kanazawa, H.; Kodama, T.; Oku, N.; Shea, K. J. *J. Am. Chem. Soc.* **2010**, *132*, 6644−6645.
(8) Bergmann, N. M.; Peppas, N. A. *Prog. Polym. Sci.* **2008**, *33*, 271−288.
(9) Gao, D.; Zhang, Z.; Wu, M.; Xie, C.; Guan, G.; Wang, D. *J. Am. Chem. Soc.* **2007**, *129*, 7859−7866.
(10) Verheyen, E.; Schillemans, J. P.; van Wijk, M.; Demeniex, M. A.; Hennink, W. E.; van Nostrum, C. F. *Biomaterials* **2011**, *32*, 3008−3020.
(11) Zhang, W.; Qin, L.; He, X. W.; Li, W. Y.; Zhang, Y. K. *J. Chromatogr., A* **2009**, *1216*, 4560−4567.
(12) Xia, Z.; Lin, Z.; Xiao, Y.; Wang, L.; Zheng, J.; Yang, H.; Chen, G. *Biosens. Bioelectron.* **2013**, *47C*, 120−126.
(13) Yang, H. H.; Zhang, S. Q.; Yang, W.; Chen, X. L.; Zhuang, Z. X.; Xu, J. G.; Wang, X. R. *J. Am. Chem. Soc.* **2004**, *126*, 4054−4055.
(14) Ouyang, R.; Lei, J.; Ju, H. *Chem. Commun.* **2008**, 5761−5763.
(15) Xu, C.; Uddin, K. M.; Shen, X.; Jayawardena, H. S.; Yan, M.; Ye, L. *ACS Appl. Mater. Interfaces* **2013**, *5*, 5208−5213.
(16) Li, Z.; Barnes, J. C.; Bosoy, A.; Stoddart, J. F.; Zink, J. I. *Chem. Soc. Rev.* **2012**, *41*, 2590−2605.
(17) Valizadeh, A.; Mikaeili, H.; Samiei, M.; Farkhani, S. M.; Zarghami, N.; Kouhi, M.; Akbarzadeh, A.; Davaran, S. *Nanoscale Res. Lett.* **2012**, *7*, 480.
(18) Yu, K.; Zaman, B.; Romanova, S.; Wang, D. S.; Ripmeester, J. A. *Small* **2005**, *1*, 332−338.
(19) Li, H.; Li, Y.; Cheng, J. *Chem. Mater.* **2010**, *22*, 2451−2457.
(20) Wang, H. F.; He, Y.; Ji, T. R.; Yan, X. P. *Anal. Chem.* **2009**, *81*, 1615−1621.
(21) Liu, H.; Fang, G.; Li, C.; Pan, M.; Liu, C.; Fan, C.; Wang, S. *J. Mater. Chem.* **2012**, *22*, 19882−19887.
(22) Zhang, W.; He, X. W.; Chen, Y.; Li, W. Y.; Zhang, Y. K. *Biosens. Bioelectron.* **2011**, *26*, 2553−2558.
(23) Zhang, W.; He, X. W.; Chen, Y.; Li, W. Y.; Zhang, Y. K. *Biosens. Bioelectron.* **2012**, *31*, 84−89.
(24) Zhang, W.; He, X. W.; Li, W. Y.; Zhang, Y. K. *Chem. Commun.* **2012**, *48*, 1757−1759.
(25) Ding, X.; Heiden, P. A. *Macromol. Mater. Eng.* **2013**, DOI: 10.1002/mame.201300160.
(26) Diltemiz, S. E.; Say, R.; Buyuktiryaki, S.; Hur, D.; Denizli, A.; Ersoz, A. *Talanta* **2008**, *75*, 890−896.
(27) Yang, P.; Zhang, L.; Li, X.; Zhang, Y.; Liu, N.; Zhang, R. *J. Non-Cryst. Solids* **2012**, *358*, 3069−3073.
(28) Li, L.; Qian, H.; Ren, J. *Chem. Commun.* **2005**, 528−530.
(29) Stöber, W.; Fink, A.; Bohn, E. *J. Colloid Interface Sci.* **1968**, *26*, 62−69.
(30) Gao, R.; Zhang, J.; He, X.; Chen, L.; Zhang, Y. *Anal. Bioanal. Chem.* **2010**, *398*, 451−461.
(31) Zhang, K.; Zhou, H.; Mei, Q.; Wang, S.; Guan, G.; Liu, R.; Zhang, J.; Zhang, Z. *J. Am. Chem. Soc.* **2011**, *133*, 8424−8427.
(32) Chen, L.; Chen, C.; Li, R.; Li, Y.; Liu, S. *Chem. Commun.* **2009**, 2670−2672.
(33) Lu, L.; Capek, R.; Kornowski, A.; Gaponik, N.; Eychmuller, A. *Angew. Chem., Int. Ed.* **2005**, *44*, 5997−6001.
(34) Lin, Z.; Xia, Z.; Zheng, J.; Zheng, D.; Zhang, L.; Yang, H.; Chen, G. *J. Mater. Chem.* **2012**, *22*, 17914.
(35) Gupta, R.; Kumar, A. *Biotechnol. Adv.* **2008**, *26*, 533−547.
(36) Xia, Y. Q.; Guo, T. Y.; Song, M. D.; Zhang, B. H.; Zhang, B. L. *Biomacromolecules* **2005**, *6*, 2601−2606.
(37) Xue, L.; Zhou, X.; Xing, D. *Anal. Chem.* **2012**, *84*, 3507−3513.